75. Shannon, C. E. A Mathematical Theory of Communication. *Bell System Technical Journal* **27,** 623–656. doi:10.1002/j.1538-7305.1948.tb00917.x (Oct. 1948).

76. Schneider, T. D., Stormo, G. D., Gold, L. & Ehrenfeucht, A. Information content of binding sites on nucleotide sequences. *Journal of Molecular Biology* **188,** 415–431. doi:10.1016/0022-2836(86)90165-8 (1986).

77. Li, W. & Godzik, A. Cd-hit: a fast program for clustering and comparing large sets of protein or nucleotide sequences. *Bioinformatics* **22,** 1658–1659. doi:10.1093/bioinformatics/btl158 (May 2006).

78. *San Diego Supercomputer Center (2022): Triton Shared Computing Cluster. University of California. Service.* https://doi.org/10.57873/T34W2R.

79. Velthuis, A. J., Long, J. S. & Barclay, W. S. Assays to Measure the Activity of Influenza Virus Polymerase. *Methods in molecular biology (Clifton, N.J.)* **1836,** 343–374. doi:10.1007/978-1-4939-8678-1_17 (2018).

Supplementary Figures, Tables, and Files

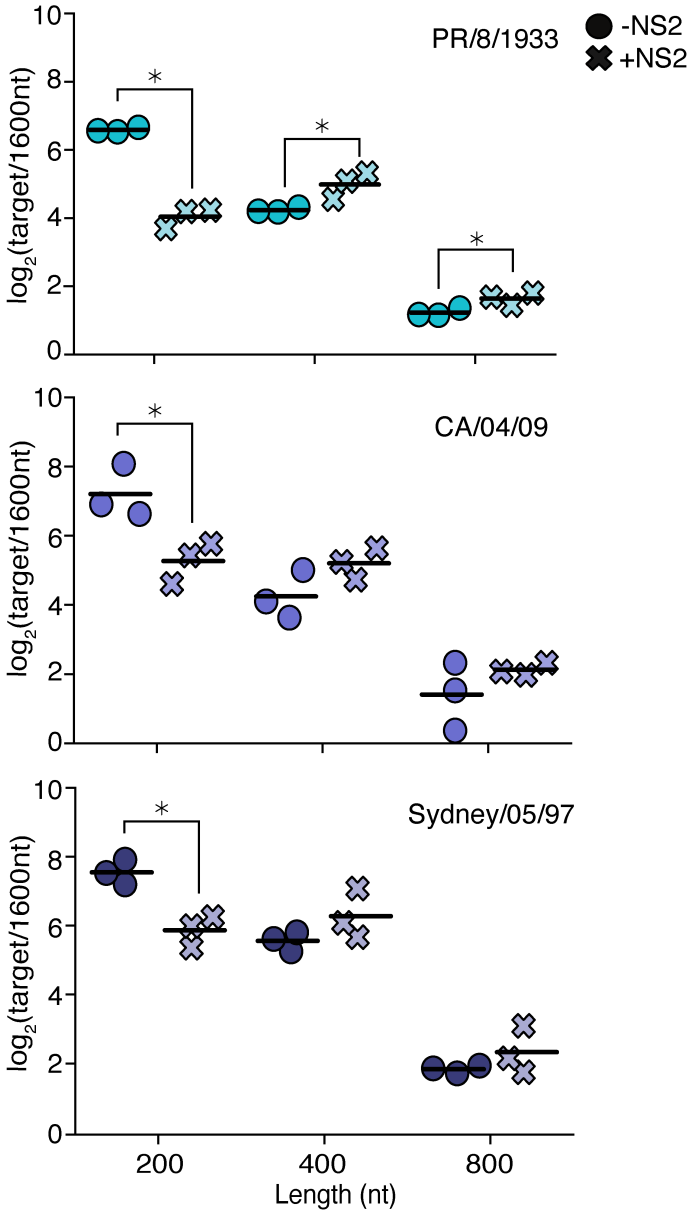

Supplementary Figure 1. NS2 expression from diverse IAV strains exhibit similar effects on genome replication.

Experiments performed as in Fig 2, using the PB1 segment and minimal replication machinery from A/WSN/1933 and NS2 from the indicated IAV strains. Asterisks indicate conditions significantly impacted by the expression of NS2, two-sample two-tailed t-test with a within-panel Benjamini-Hochberg corrected FDR<0.05. n=3, individual replicates and mean displayed.

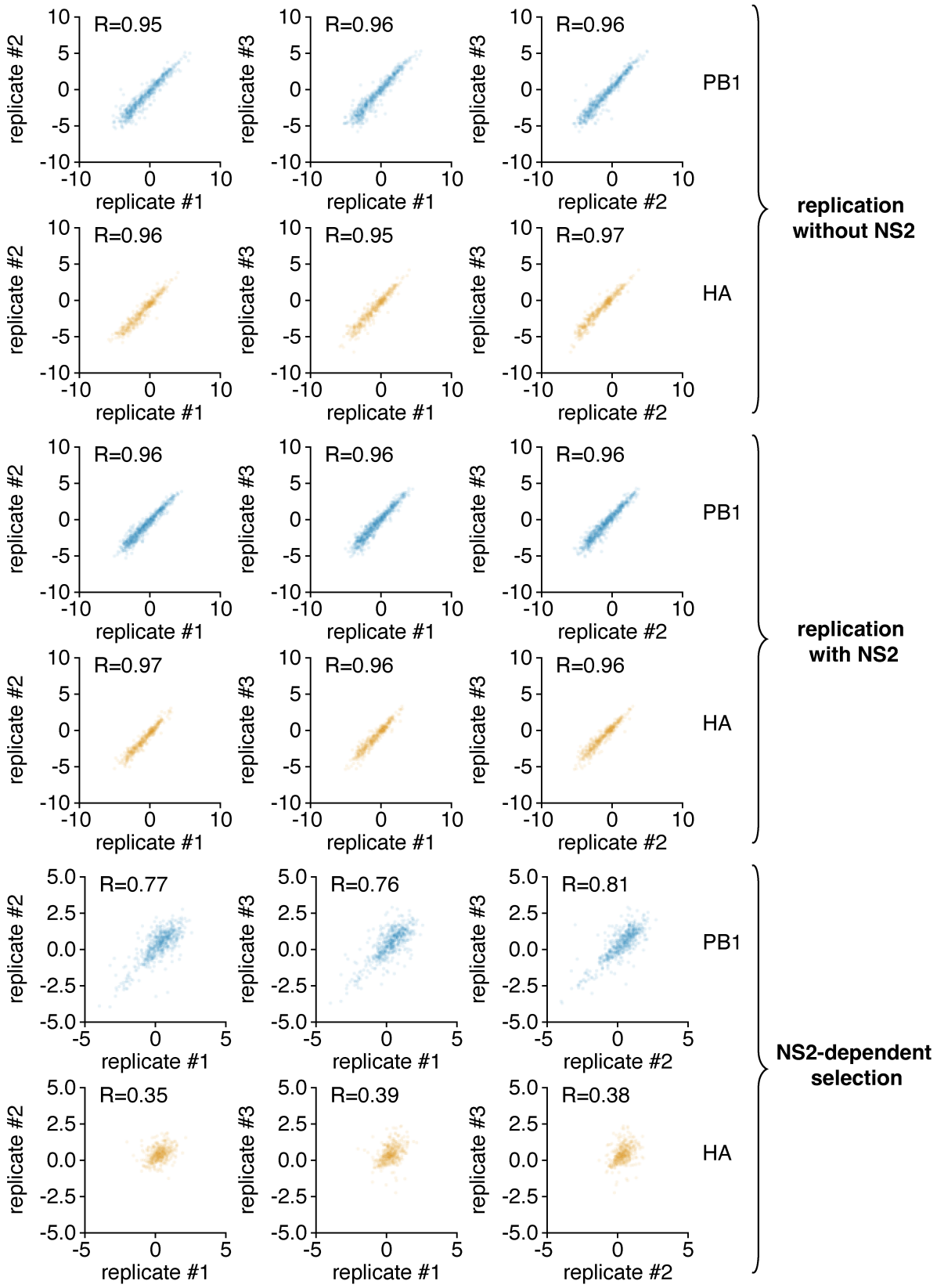

Supplementary Figure 2. Inter-replicate correlation from Fig. 3.
Inter-replicate enrichment or depletion values as calculated in Fig 3. Values are in $\log_2$. R is the Pearson correlation coefficient.

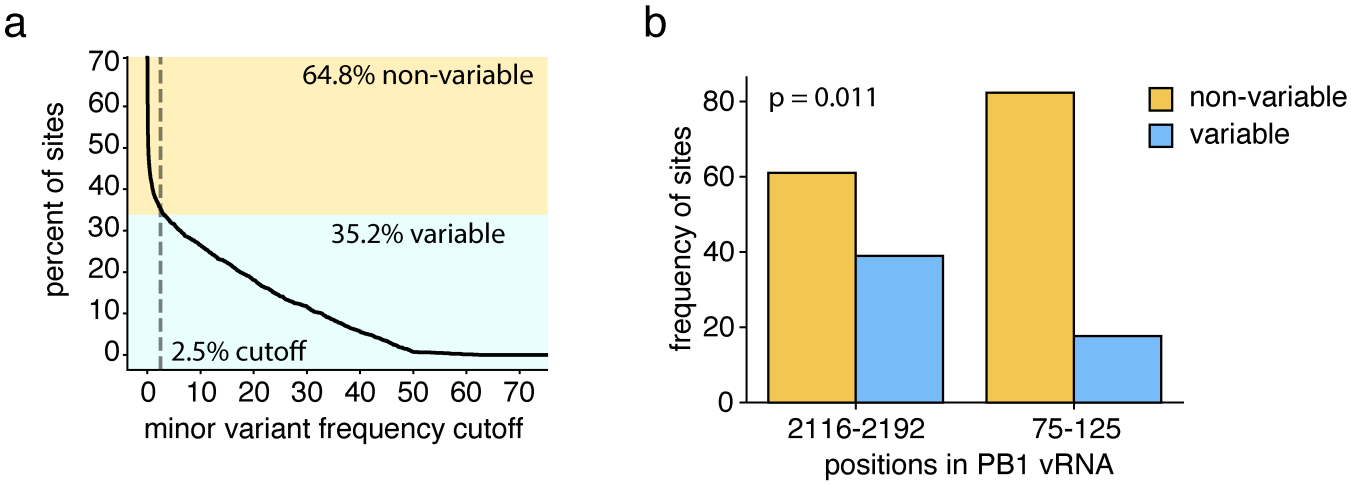

Supplementary Figure 3. Conservation of regions from Fig. 4c across natural PB1 sequences. To compare natural diveristy, we procured PB1 sequences from the NCBI flu database on July 25th, 2024 that met the following prerequisites: full-length, 2341nt long, and exclude vaccine and laboratory strains. These sequences were then clustered by CD-HIT to an identity of 99%, and a single example of each cluster retained. Thereafter, sequences with ambiguities or indels relative to other PB1 sequences, were manually removed. This rsulted in 1939, high-quality, PB1 sequences that exhibit good alignment when simply lined-up with one-another, giving high confidence in the comparability of any given position, and, given the CD-HIT clustering, are unlikely to be aggressively weighted towards any single outbreak. **a** To define positions as variable or non-variable, we calculated the fraction of variable sites depending on the minimum minor variant frequency at which we consider a position variable. For instance, at the chosen cutoff, 2.5%, a position is considered variable if at least 2.5% of sequences do not match the major variant at that site. This cutoff was chosen to match the inflection point on our curve. **b** Frequency of variable sites within the given regions of PB1 as defined in 4c. Significant difference tested using Fisher's exact test, p value shown.

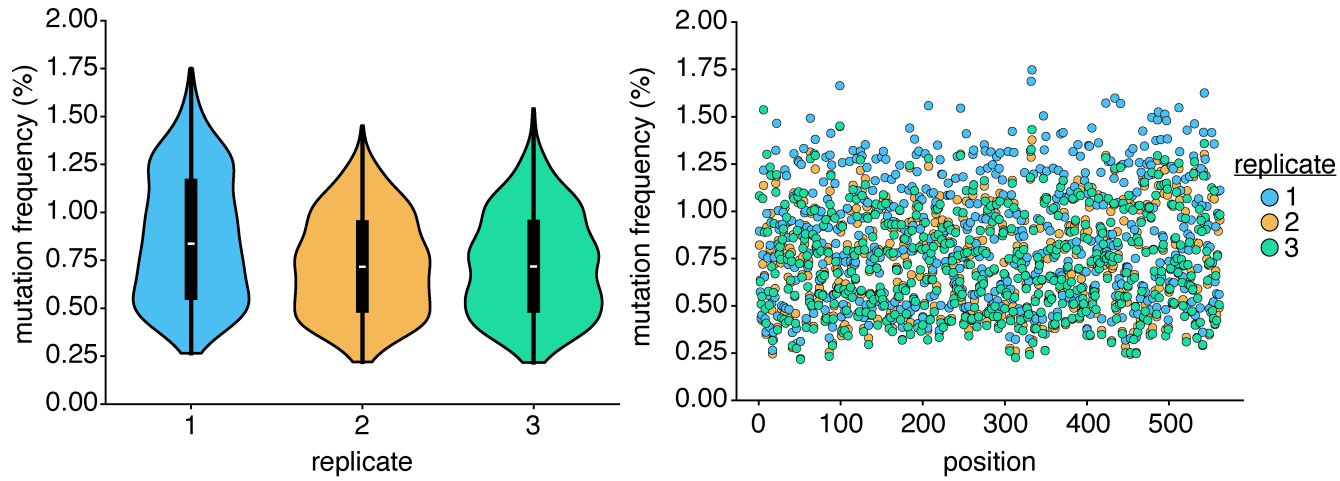

Supplementary Figure 4. Generation of single-nucleotide variant libraries in $PB1_{177:385}$. (left) Per site Mutation frequency as measured by Illumina sequencing of $PB1_{177:385}$ libraries generated by mutagenic PCR across each of the three replicate libraries. Libraries were relatively uniform, with a median mutation frequency ranging from 0.716% to 0.836% (right) Data from (left) displayed per individual site in $PB1_{177:385}$. Mutation rate was relatively uniform across this template, with no particular regions exhibiting particularly aberrant frequencies across three replicates.

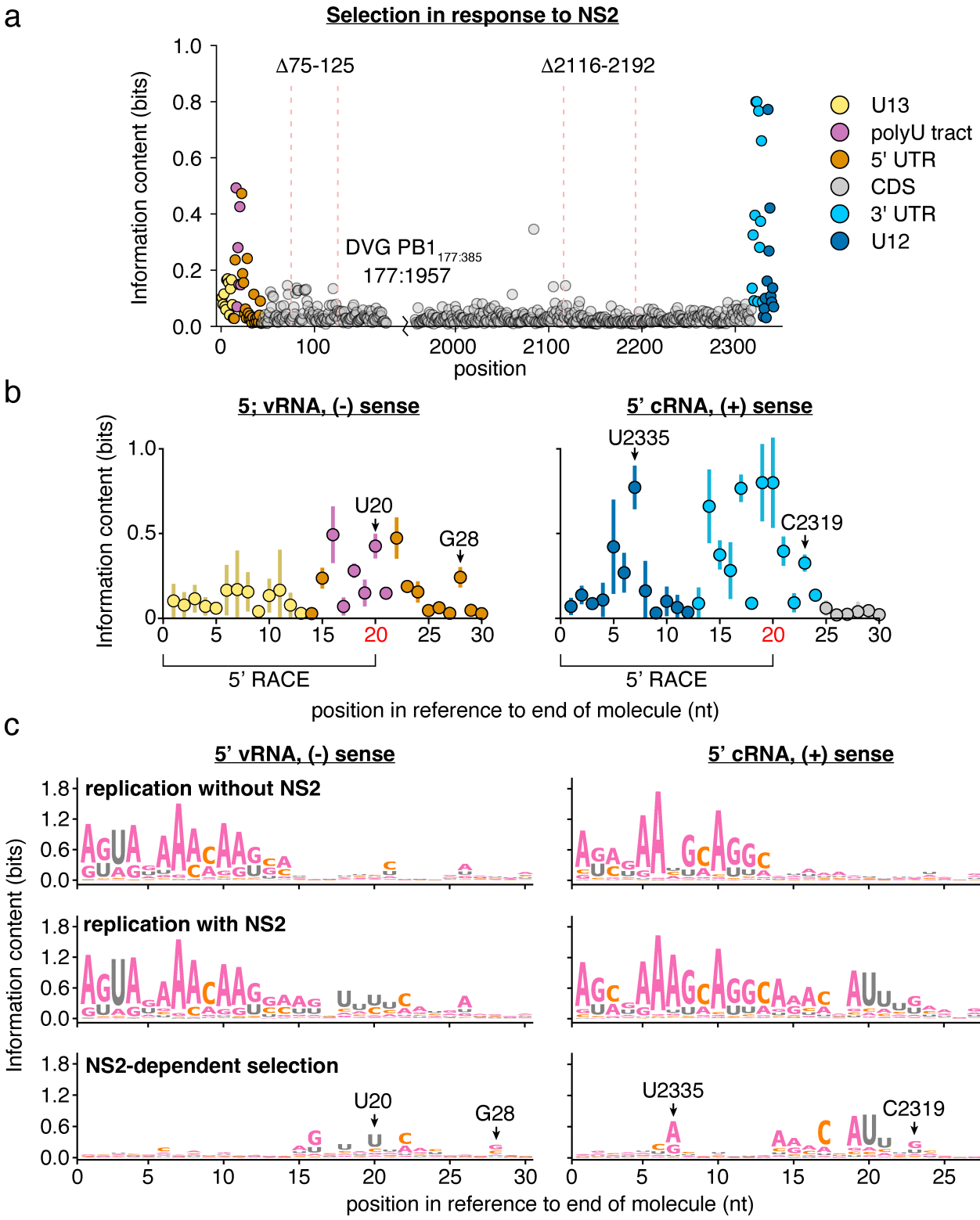

Supplementary Figure 5. Information content of single-nucleotide variant libraries in $PB1_{177:385}$. Information content calculated using Shannon entropy of the selection preferences at each position. Sequence logos generated by assigning this information content to each nucleotide in order of the strength of selection. **a** Information content analysis of data as presented in Fig. 5a. Each point represents the average of three replicates. **b** Information content analysis of data as presented in Fig. 5b, for NS2-dependent selection only. Mean and standard deviation displayed, n=3. Positions chosen for further analysis in Fig. 6 noted. **c** Sequence logo plots for positions displayed in Fig 5b. Data presented are the median values across three replicates. Positions chosen for further analysis in Fig. 6 noted. Inter-replicate correlation plots presented in (Supplementary Fig. 6)

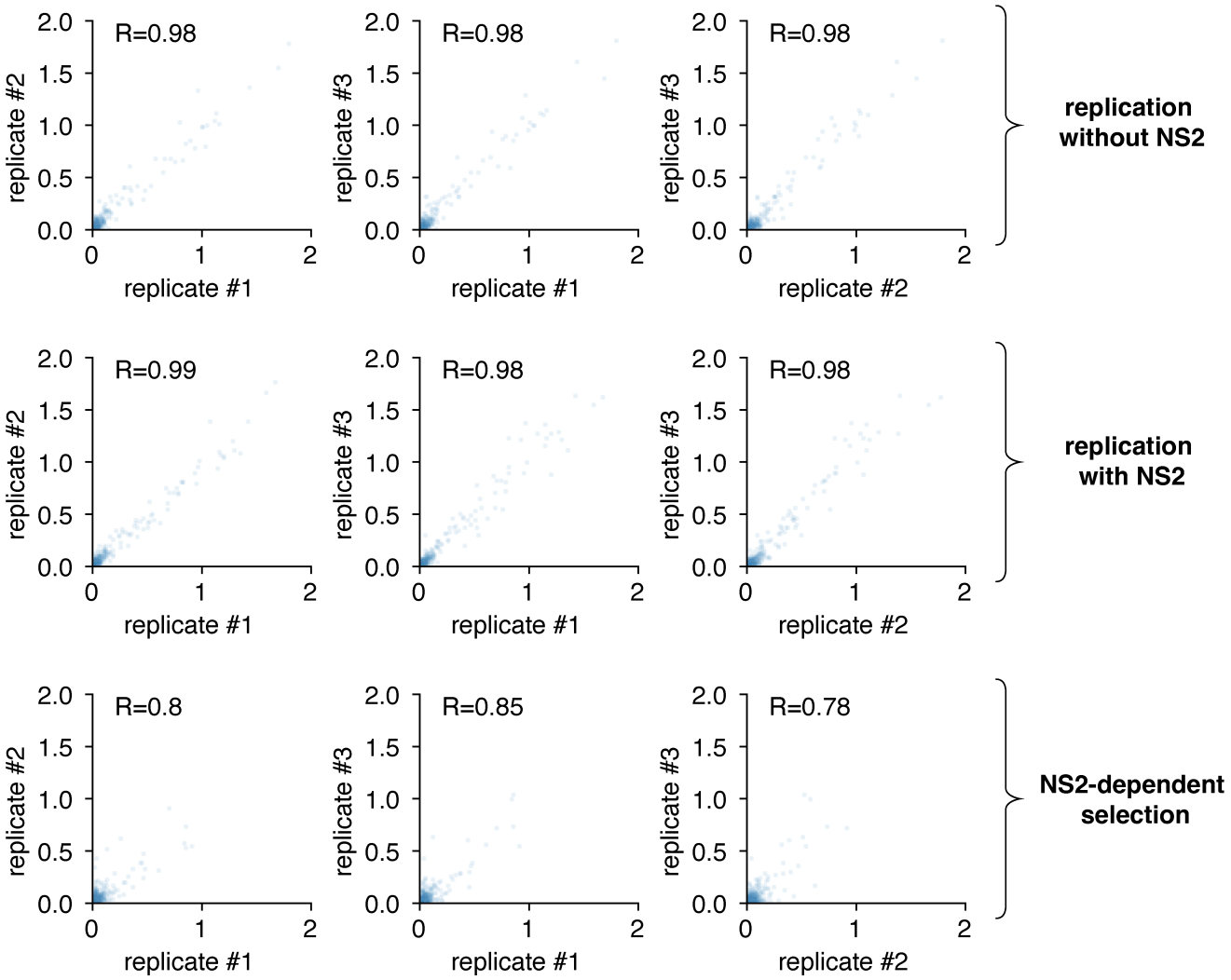

Supplementary Figure 6. Inter-replicate correlation from Supplementary Fig. 5.
Inter-replicate information content (total) values as calculated in Supplementary Fig 5. Values are in bits. R is the Pearson correlation coefficient.

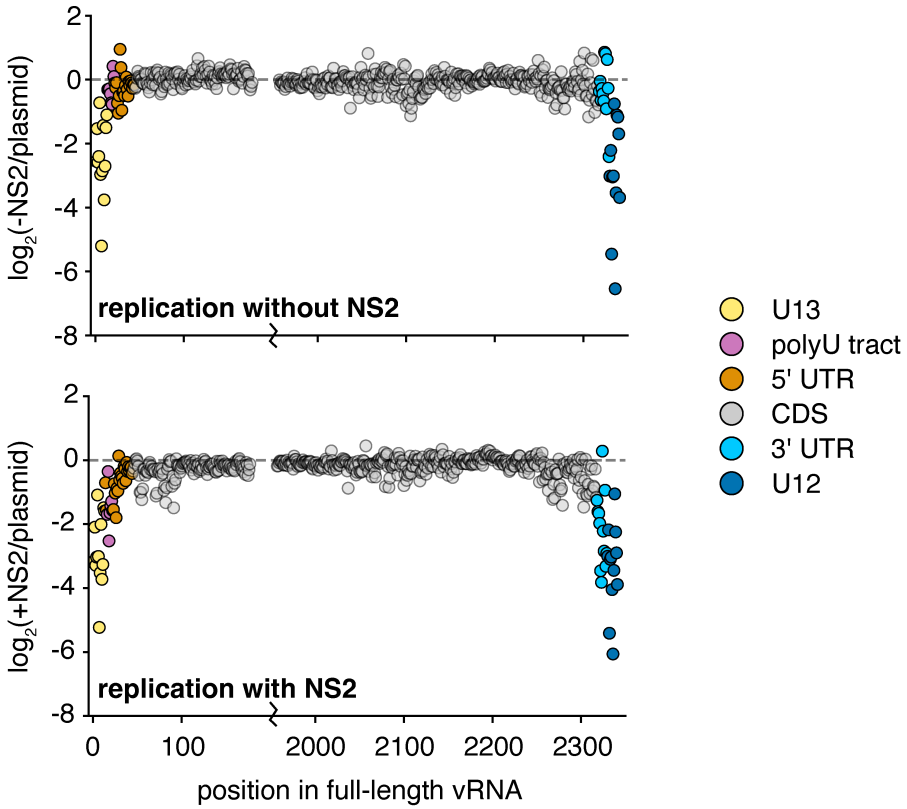

Supplementary Figure 7. Full-length selection of subsets shown in Fig. 5b.
Selection measured under each condition across all of $PB1_{177:385}$ against non-wild-type nucleotides, average value across all three replicates provided.

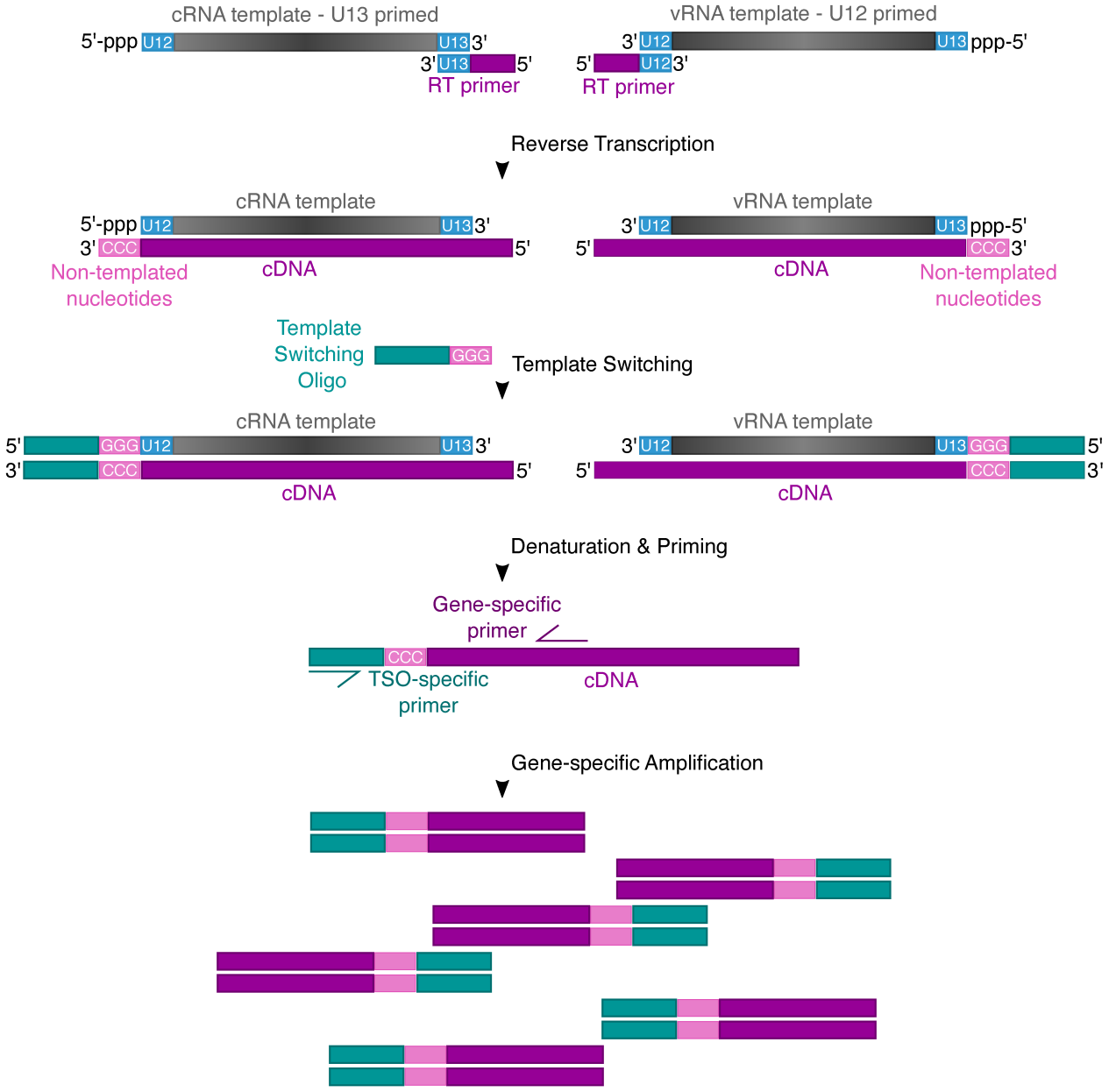

Supplementary Figure 8. RACE inference of 5' sequence.
Schematic depicting the process by which 5' sequence of cRNA and vRNA were measured.

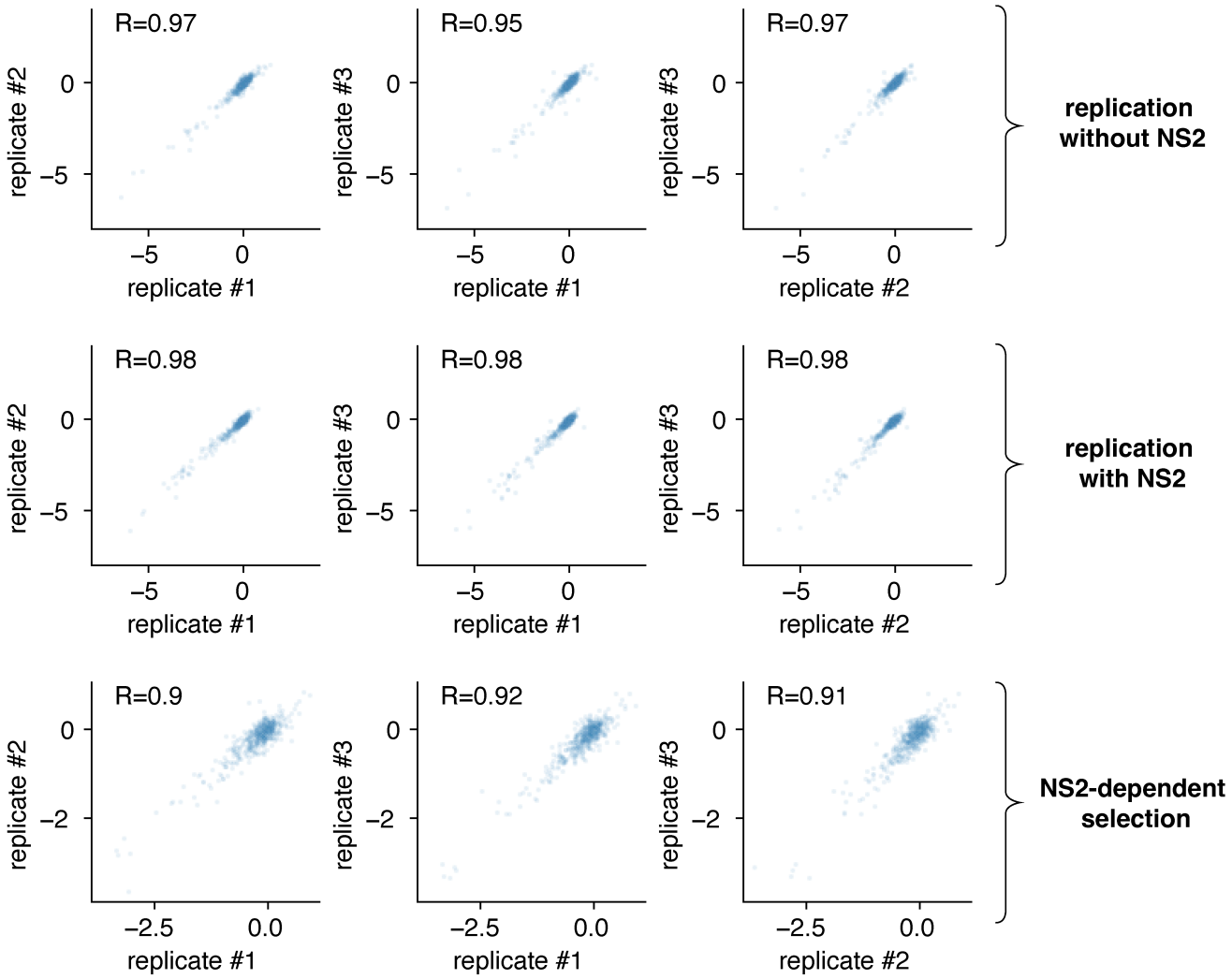

Supplementary Figure 9. Inter-replicate correlation from Fig. 5.
Inter-replicate selection on non-wild-type nucleotides as calculated in Fig 5. Values are in $\log_2$. R is the Pearson correlation coefficient.

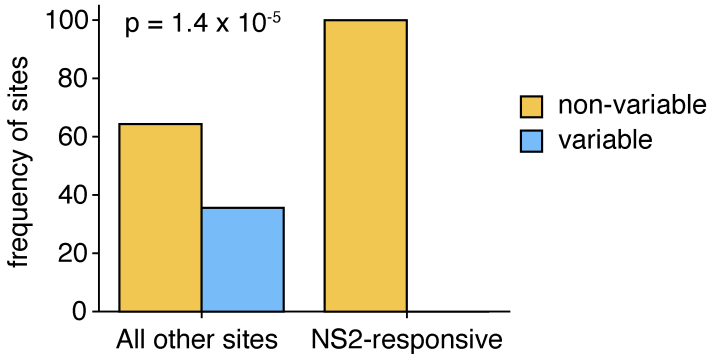

Supplementary Figure 10. Conservation of sites identified in Fig. 5a as NS2-responsive across natural PB1 sequences.
Analysis performed as in Supplementary Fig. 3 comparing the 27 sites we identify as critical to replication in the presence of NS2 as compared to all other sites in PB1. These sites are listed in Supplementary Table 1. Significant difference tested using Fisher's exact test, p value shown.

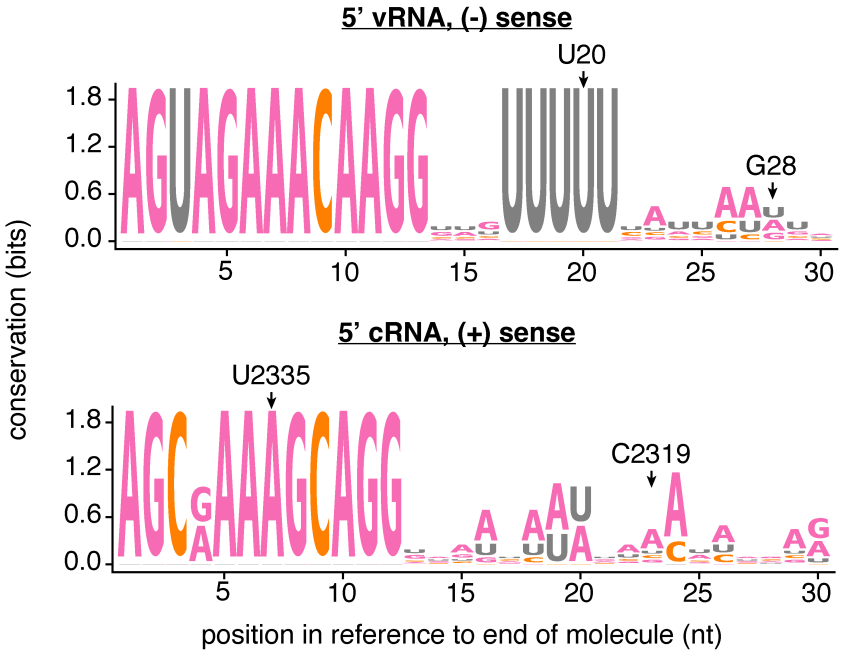

Supplementary Figure 11. NS2 responsive sites are not identical between IAV segments.
The first 30nt of the vRNA and cRNA were compared between the eight IAV segments, and sequence logo plots generated. The sites we tested in Fig. 6 are highlighted.

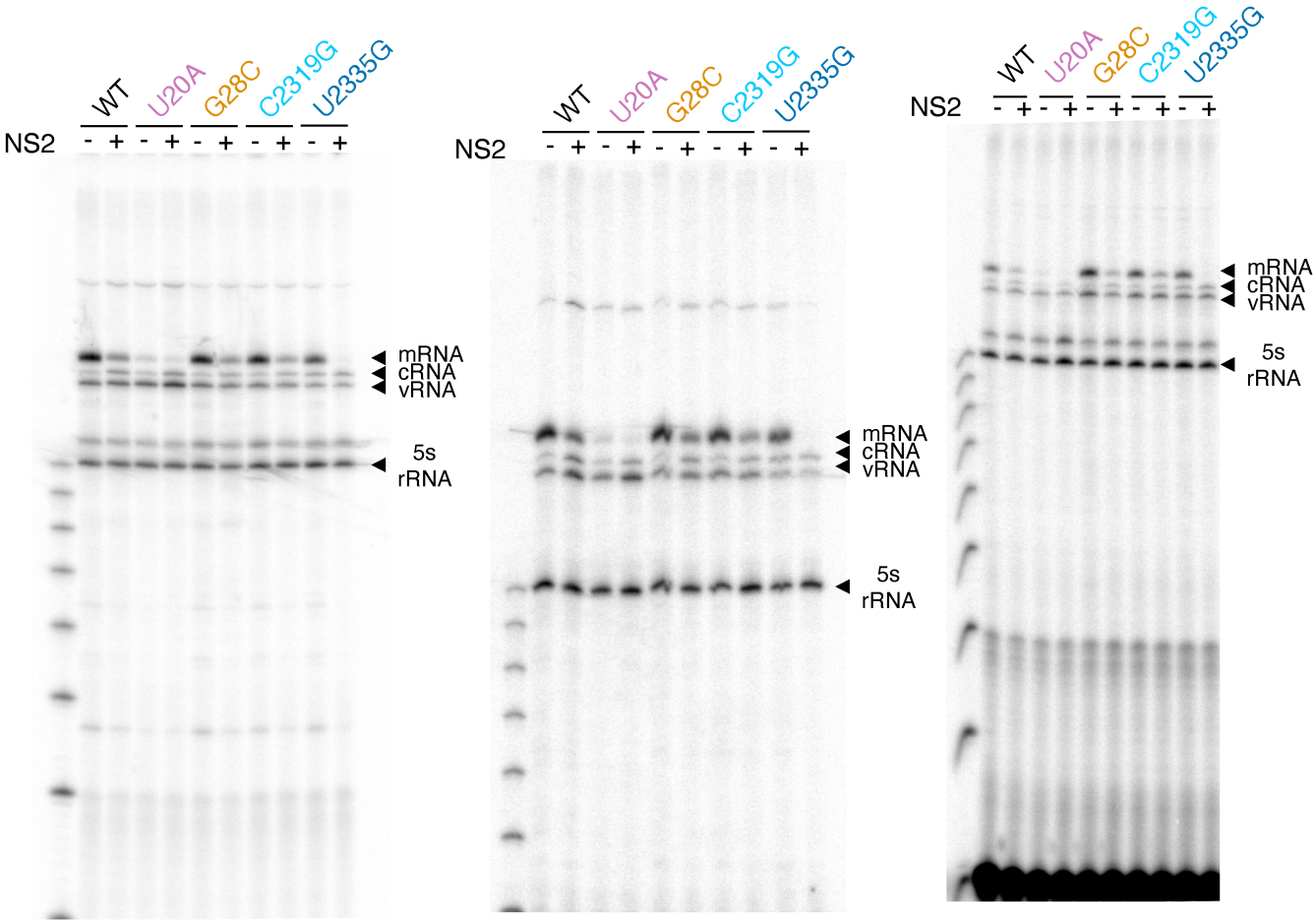

Supplementary Figure 12. Primer extension analysis of various $PB1_{177:385}$ variants in minimal replication assays with, and without, NS2.
Full gels from primer extension analysis presented in Fig. 6b,c. First gel is the gel presented in Fig. 6b.

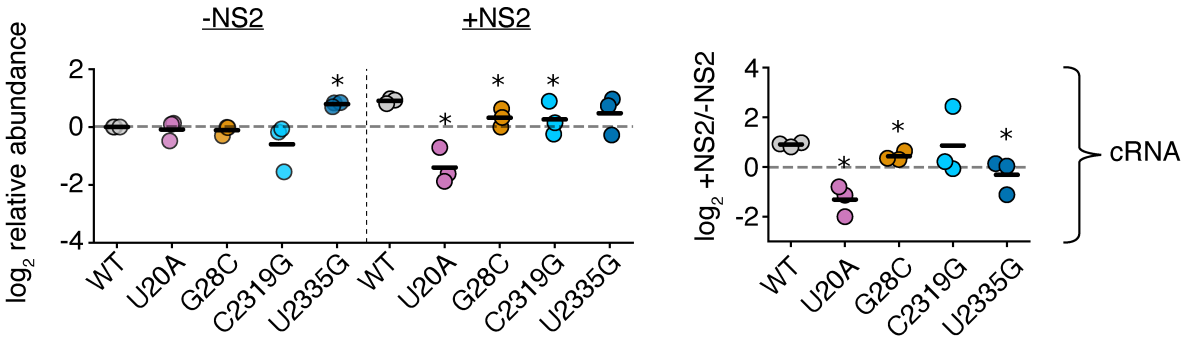

Supplementary Figure 13. Mutations to NS2-dependent sites can impact replication of cRNA in full-length PB1

For all experiments, the canonical start codon was removed by mutagenesis to remove effects of additional expression of PB1. Quantitative analysis of primer extension as presented in Supplementary Fig. 14. All values in left two columns corrected against a parental template in the absence of NS2. Dotted line represents that value, points above indicate an increase in that molecular species, below, decrease. Values in the right column represent the ratio of points between the left two columns. Asterisks indicate values that are significantly decreased relative to the parental template, one-tailed t-test with Benjamini-Hochberg corrected FDR <0.1. Full gels presented in Supplementary Fig. 14. Individual replicates and mean presented, n=3.

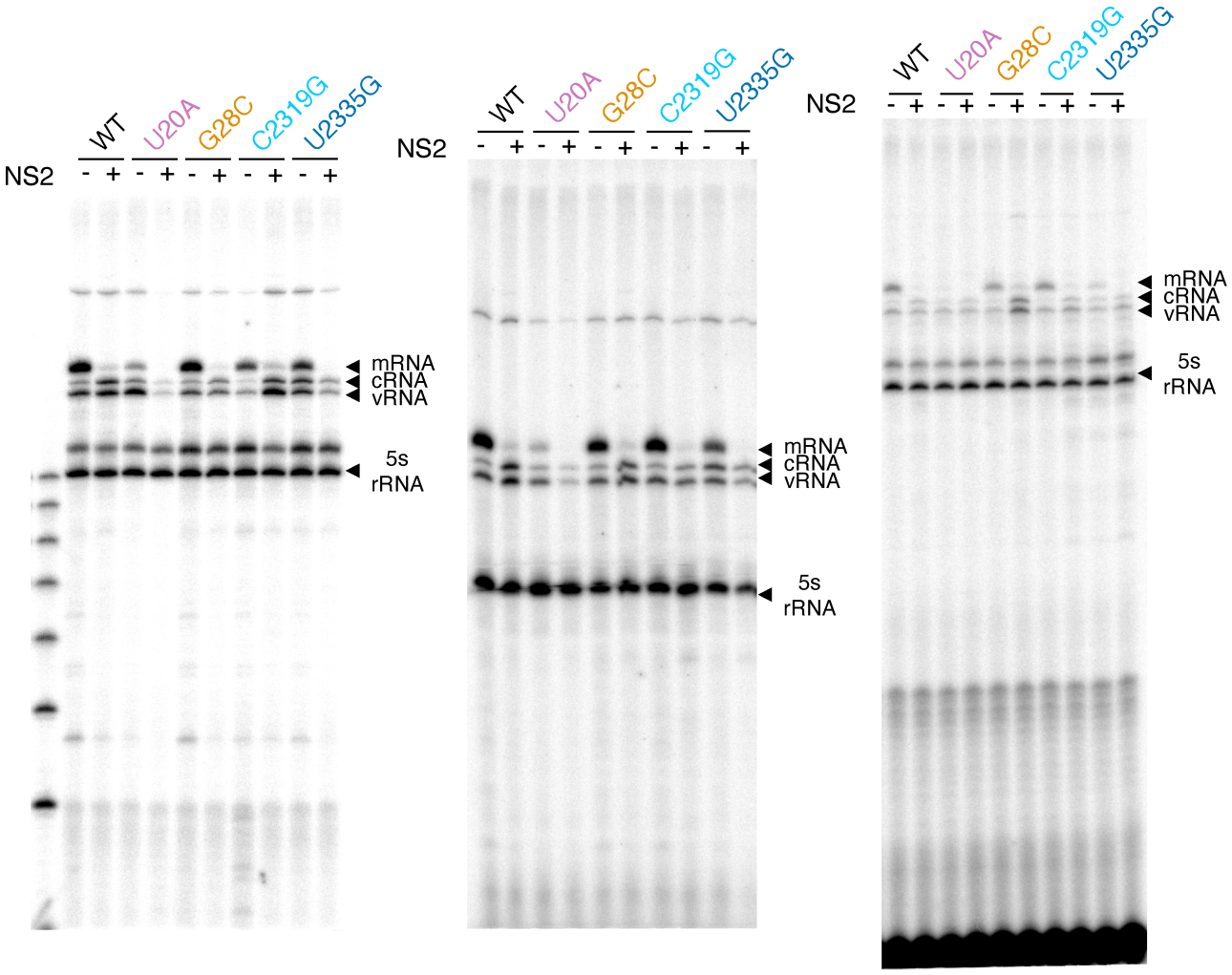

Supplementary Figure 14. Primer extension analysis of various full-length PB1 variants in minimal replication assays with, and without, NS2.
Full gels from primer extension analysis presented in Supplementary Fig. 13.

context	Nucleotide position (vRNA)	log2 NS2-dependent effect	pval	qval
5' UTR	15	-1.26642623	0.0053062	0.05516478
polyU	16	-1.407887837	0.00580593	0.05530393
polyU	18	-1.795893957	0.00826029	0.06727946
polyU	20	-1.844711513	0.00254884	0.04325913
polyU	21	-1.37795038	0.00446839	0.05022535
5' UTR	22	-1.462633616	0.02373645	0.09737143
5' UTR	23	-1.285950966	0.01276786	0.07827812
5' UTR	28	-1.90659152	0.0048643	0.05257184
CDS	55	-1.101661611	0.00234029	0.04286222
CDS	56	-1.100544239	0.00189633	0.04232093
CDS	71	-1.326675414	0.01338237	0.07827812
CDS	72	-1.03733307	0.0000459	0.01290355
CDS	82	-1.178798373	0.0111679	0.07659062
CDS	83	-1.067901354	0.00338681	0.04531879
CDS	91	-1.372475945	0.00471253	0.05193021
3' UTR	2319	-1.555944694	0.00131708	0.03949276
3' UTR	2320	-1.015444989	0.02231737	0.09582604
3' UTR	2321	-1.696175204	0.0130107	0.07827812
3' UTR	2322	-3.011824531	0.0084403	0.06776352
3' UTR	2323	-3.149977188	0.00244055	0.04286222
3' UTR	2325	-3.02907342	0.00132183	0.03949276
3' UTR	2326	-1.928677286	0.02540826	0.09776512
3' UTR	2327	-1.56234586	0.00266523	0.04325913
3' UTR	2328	-3.048000255	0.00326677	0.04477866
U12	2335	-3.286629043	0.00325948	0.04477866
U12	2339	-1.072209116	0.0008218	0.03949276
U12	2340	-1.19881869	0.01855345	0.09035903

Supplementary Table 1. NS2-responsive sites.
Table of all sites identified as meeting significance from Fig 5a.

Supplementary Data 1. Genome sequence of A/WSN/1933.
Genome sequence of A/WSN/1933 used in this study.

Supplementary Data 2. $PB1_{177:385}$ sequence.
Sequence of $PB1_{177:385}$ from this study.

Supplementary Data 3. NS2 sequences.
NS2 sequences used in this study.

Supplementary Data 4. Primer list.
List of all primer sequences used in this study.

Supplementary Data 5. PB1 sequences.
PB1 sequences used to assess natural diversity.